European Association for the Development of Renewable Energies, Environment and Power Quality (EA4EPQ)

International Conference on Renewable Energies and Power Quality (ICREPQ'10)
Granada (Spain), 23rd to 25th March, 2010

A Comparative Study on Variable-Speed Operations of a Wind Generation System Using Vector Control

A.J. Mahdi, W.H. Tang, L. Jiang and Q.H. Wu
Department of Electrical Engineering and Electronics
The University of Liverpool, Liverpool, L69 3GJ, U.K.
E-mail: whtang@liv.ac.uk

Abstract. This paper presents a comparison study among three control methods based on vector control for maximising the output power and improving the performance of a small-scale wind generation system (WGS). The three control methods are a hysteresis-band current controller (HBCC), a PI current controller (PICC) and an improved PI current controller (IPICC) which is based on particle swarm optimisation (PSO). The WGS investigated in this research consists of a permanent magnet synchronous generator (PMSG) directly driven by a vertical-axis wind turbine (VAWT), a current controlled PWM rectifier, and a stand-alone DC load. The principle of maximum power point tracking (MPPT) is to adjust the rotational speed of a wind turbine at optimal speeds that ensures optimal tip-speed ratios (TSR) and maximum power coefficients over a wide range of wind speeds. Simulations are based on actual parameters which are obtained experimentally from a real wind turbine generator system. The simulation results show the effectiveness of the IPICC method compared with the HBCC and PICC methods due to its satisfactory dynamic responses with fast MPPT under wind speed variations.

Key Words

Variable-speed wind generation systems, maximum power point tracking, vector control, permanent magnet synchronous generator, controlled PWM rectifiers.

1. Introduction

WGS is efficient for a stand-alone hybrid power generation system and a cost effective solution for street lighting utilities. The optimal operation of a WGS is important due to the high initial cost and the low efficiency of the wind turbine generator systems. There are many factors that contribute to increasing wind turbine efficiencies, including the number of rotor blades, a blade pitch angle, and TSR which is the ratio of circumstantial speed to wind speed. In a small-scale WGS, the only possible control variable for yielding the maximum amount of energy from wind is TSR by adjusting the rotational speed to a reference value in order to keep TSR at its optimal value and consequently the power coefficient at its maximum value [1].

Operations of WGS can mainly be classified into two types: (i) a constant-speed wind turbine is based on adjusting the pitch angle of wind turbine blades in order to control the output power of a wind turbine. (ii) a variable-speed wind turbine operated by controlling the rotational speed of a wind turbine according to a reference speed that ensures the optimal TSR and a maximum power coefficient.

In general, MPPT techniques can be classified into two main categories. The first one is based on the knowledge of wind turbine characteristics which is the power coefficient versus TSR curve, and the second method is rooted on estimating the optimal reference signals of a control system [2]. Vector control strategies have been widely used for PMSG using a PWM controlled rectifier and PWM inverter. Basically, the aim of a vector control strategy for the generator-side is to control MPPT by changing the speed of the wind turbine. The overall control system consists of two main control loops: (i) a speed controller compares the reference speed (which is calculated from a TSR controller) with a PMSG speed and generates a reference torque, (ii) current controllers compare the reference dq-axis currents with the PMSG dq-axis currents to generate switching signal for a PWM current controller. The aim of the vector control strategy for a grid side PWM inverter is to maintain the DC link voltage constant regardless of the amount of the generator power, while keeping sinusoidal grid currents [3].

This paper is organised as follows. In Section 2, the models of a wind turbine and a PMSG are presented. Section 3 illustrates the three control methods, which are based on the vector control strategy: decoupling control method, i.e. HBCC method, PICC method and IPICC method. Simulation results are presented in Section 4. Finally, some conclusions are presented in Section 5.

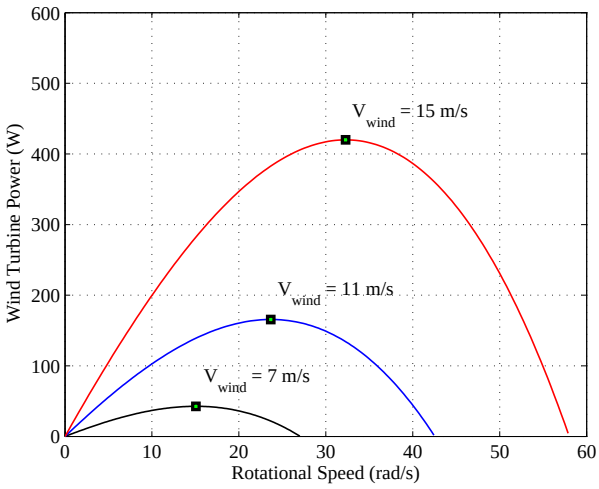

Fig. 1. VAWT characteristics

2. Modeling of the WGS

A. Wind Turbine Model

The kinetic energy in wind is related to the cube of the wind speed. The available wind power P_w is [4]

$$P_w = 0.5\rho A V_{\text{wind}}^3, \tag{1}$$

where ρ is wind density, A the wind turbine swept area, and V_{wind} the wind speed. The extracted mechanical power P_m using a wind turbine from the available wind power P_w is calculated with the power coefficient C_p as follows

$$P_m = 0.5\rho C_p A V_{\text{wind}}^3. \tag{2}$$

VAWT is widely used for small-scale wind generations due to its attractive features, which are omni-directionality and easy to maintain. To control the mechanical power of a wind turbine, it is important to keep C_p at its maximum value. The maximum C_p can be achieved by adjusting the tip speed ratio λ at its optimal value as a result of controlling the rotational speed of the wind turbine. A number of numerical approximations have been developed to calculate C_p [5]. In this research, a nonlinear empirical interpolation to represent the C_p is employed as follows:

$$\begin{cases} C_p = -0.13\lambda^3 - 0.12\lambda^2 + 0.45\lambda \\ \lambda = \frac{\omega_m R}{V_{\text{wind}}} \end{cases} \tag{3}$$

where R is the radius of the wind turbine rotor and ω_m the mechanical rotational speed. Figure 1 shows the calculated wind turbine characteristics used in this research. It can be seen there is one specific rotational speed at which the output power of the wind turbine is maximum.

B. Dynamic Model of PMSG

The model of a PMSG is represented in the dq-axis frame which is widely used. In the dq-axis frame, the d-axis is aligned with the magnet axis and the q-axis is orthogonal to the d-axis. The dq-axis model of a PMSG is described as follows [6], [7]:

Table I

PMSG MODEL VARIABLES AND PARAMETER DEFINITION

Symbol	Definition	Unit
v_s	Phase voltage	V
i_s	Phase current	A
Ψ_s	Phase flux linkage	Wb
ω_e	Electrical rotational speed	rad/s
ω_m	Mechanical rotational speed	rad/s
T_e	Electromagnetic torque	N.m
T_{wt}	Wind turbine torque	N.m
θ_m	Mechanical position angle	rad
i_d	d-axis current	A
i_q	q-axis current	A
v_d	d-axis voltage	V
v_q	q-axis voltage	V
Ψ_d	d-axis flux linkage	Wb
Ψ_q	q-axis flux linkage	Wb
R_s	Phase resistance	Ω
L_d	d-axis inductance	mH
L_q	q-axis inductance	mH
λ_{PM}	PM flux linkage	mWb
J	Inertia	kg.m^2
F	Viscus friction	N.m/rad.s
p	Pole pairs	-

$$-v_s = i_s R_s + \frac{d\Psi_s}{dt} + jw_e\Psi_s \tag{4}$$

$$\frac{d}{dt}\omega_m = \frac{1}{J}(T_e - T_{\text{wt}} - F\omega_m) \tag{5}$$

$$\frac{d}{dt}\theta_m = \omega_m \tag{6}$$

$$\omega_e = p\omega_m \tag{7}$$

$$\theta_e = p\theta_m \tag{8}$$

$$T_e = 1.5p(\lambda_{\text{PM}} i_q + (L_d - L_q) i_q i_d) \tag{9}$$

The space vector variables of the PMSG model are:

$$\begin{cases} v_s = v_d + jv_q \\ \Psi_s = \Psi_d + j\Psi_q \\ \Psi_d = \lambda_{\text{PM}} + L_d i_d \\ \Psi_q = L_q i_q \\ i_s = i_d + j i_q \end{cases} \tag{10}$$

where all the PMSG model variables and parameter definitions are listed in Table I. Thus, the PMSG dynamic equations are given by:

$$\frac{d}{dt} i_d = \frac{1}{L_d}(V_d - R_s i_d + L_q \omega_e i_q) \tag{11}$$

$$\frac{d}{dt} i_q = \frac{1}{L_q}(V_q - R_s i_q - L_d \omega_e i_d - \lambda_{\text{PM}}\omega_e) \tag{12}$$

In this paper, no-load and load tests have been conducted to calculate the physical parameters of a PMSG (type GL-PMG500A). The following assumptions have been made in these tests: the magnetic circuit is assumed to be linear, (i.e. magnetic saturation is neglected) and the mathematical model is without considering core losses.

3. Control of The WGS

A. Vector Control Strategy

The principle of vector control is to adjust PMSG rotational speeds according to an optimal reference speed. The rotational speed is controlled by changing the electromagnetic torque of the PMSG via dq-axis currents. In this control, the d-axis reference current is set as zero in order to avoid the demagnetisation of rotor permanent magnets, to linearise the relationship between the electromagnetic torque and the stator current which is only equal to the q-axis current, and to decrease the copper losses in a stator winding. The vector control strategy can be summarised as follows [8]:

- In the generator side, the stationary three-phase currents (a, b and c) is converted to stationary two-phase currents (alpha and beta) via the Clark transformation. In the controller side, the stationary two-phase currents is converted to dq-axis rotational currents via the Park transformation. These transformations need the shaft position of the PMSG which is measured via an encoder.
- As mentioned before, the d-axis current is kept as zero.
- The q-axis reference current is proportional to the speed reference that is generated from a TSR controller and the speed reference varies under wind speed variations.
- The vector current equals only the q-axis current which is controlled to vary the PMSG rotational speed via a PWM voltage source inverter (VSI) for each wind speed.

One of the difficulties in this control strategy is the requirement to fix an anemometer close to wind turbine blades in order to obtain accurate wind speed measurements, otherwise inaccurate calculations of the reference rotational speed is obtained causing the WTG system not to rotate at an optimal speed.

B. Decoupling Control Strategy

A decoupling function is added in the vector controller in order to linearise the PMSG model by removing cross-coupling between the dq-axis voltages. The dynamic equations of PMSG (11) and (12) can be rewritten as follows:

$$V_d = R_s i_d + \frac{d}{dt} L_d i_d - \omega_e L_q i_q \tag{13}$$

$$V_q = R_s i_q + \frac{d}{dt} L_q i_q + \omega_e (L_d i_d + \lambda_{\mathrm{PM}}) \tag{14}$$

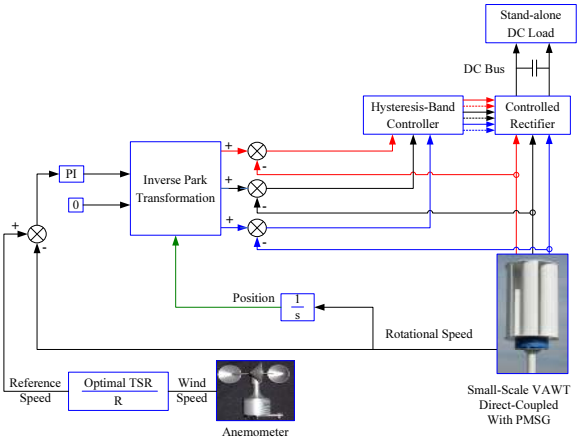

Fig. 3. A small-scale WGS controlled by the HBCC technique

It can be seen from equations (13) and (14) that cross-coupling between the dq-axis voltages are by the terms $-\omega_e L_q i_q$ and $\omega_e(L_d i_d + \lambda_{\mathrm{PM}})$ for the d-axis and q-axis respectively. Thus, the dq-axis voltage equations without cross-coupling can be written as below:

$$V_d = R_s i_d + \frac{d}{dt} L_d i_d \tag{15}$$

$$V_q = R_s i_q + \frac{d}{dt} L_q i_q \tag{16}$$

The closed-loop s-plane transfer function of the PMSG with a PI controller is calculated as the following:

$$\frac{i_d(s)}{i_{\mathrm{dref}}(s)} = \frac{k_{pd} s + k_{id}}{L_d s^2 + k_{pd} R_s s + k_{id}} \tag{17}$$

where k_{pd} and k_{id} are the proportional and integral parameters of the PI current controller.

C. Hysteresis-Band Current Control Technique

In the HBCC technique, three-phase line currents are compared with stationary three-phase reference currents to generate a current error Δi_o, which is applied to a current controller constituting a hysteresis loop to generate variable-frequency PWM pulses. The characteristics of HBCC can be represented as [10]:

$$a = \begin{cases} 0 & \text{if } \Delta i_o < -h/2 \\ 1 & \text{if } \Delta i_o > +h/2 \end{cases},$$

where h is the width of the loop and a a variable. Figure 3 shows the block diagram of a WGS controlled by HBCC technique. It is important to note that the pulses used to drive the controlled rectifier are of variable frequency because the current variations are limited from the upper to the lower level and vice versa. HBCC has a fast response to rapid variations in reference currents with a small delay.

D. PI Current Control Technique

In the PICC technique, the dq-axis currents are compared

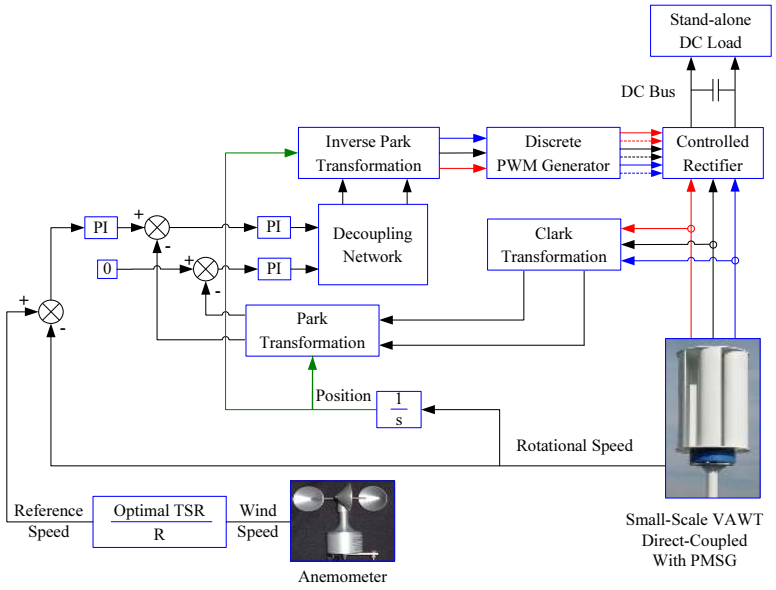

Fig. 2. A small-scale WGS controlled by the PICC technique

with dq-axis reference currents to generate dq-axis reference voltages. These voltages are linearised by decoupling voltages to generate voltage references which are then transformed into PWM pulses to drive a controlled PWM rectifier. It is important to note that the purpose of decoupling voltages is firstly to remove the effect of cross-coupling between the dq-axis current equations and secondly to improve system dynamic performances. In this technique, the PI controllers are tuned manually or by using a conventional method, *e.g.* the pole-zero placement method which is used in this research. The current loops require two PI controllers which are designed in the dq-axis rotating reference. In this reference, the dq-axis currents are converted into DC values as in a steady state. Hence, PI controllers are used to control dq-axis currents, which also decrease steady state errors to zero because of an integral part. The PI controller in the time domain is:

$$u(t) = k_p e(t) + k_i \int_{t_o}^{t} e(\tau) d\tau \tag{18}$$

where $u(t)$ is the output signal, $e(t)$ the error signal, k_p and k_i the proportional and integral coefficients respectively. The PI controller equation can be represented in the s-domain, and as a result the transfer function of the PI controller becomes:

$$TF = \frac{u(s)}{E(s)} = k_p + \frac{k_i}{s} = \frac{k_p s + k_i}{s}. \tag{19}$$

The parameters of the PI controller must be optimally calculated in order to achieve required specifications, which are:

- Minimise the closed loop current overshoots, because the generated current overshoot peaks may damage power converters in hard conditions.
- The dq-axis currents must settle within speed sampling period.

In this study, the zero and pole placement method is used. This method is applied to decrease the closed loop overshoot by placing the poles and the zeros of the control system in the same position of the s plane.

E. Improved PI Current Control Technique

In the IPICC technique, PI controllers are optimally tuned using a particle swarm optimisation (PSO) without knowing PMSG parameters. PSO is an optimisation method which is an evolutionary calculation strategy in nature motivated by the simulation of social activities. The PSO strategy can be summarised as follows [11].
Step 1: The population (swarm) is initialised with random position x and velocity v.
Step 2: The fitness value F of each particle is evaluated.
Step 3: The solution of the fitness value is verified as follows:

$$\begin{cases} if F(x) > f(g_{\text{best}}) \\ g_{\text{best}} = x \\ if F(x) > f(p_{\text{best}}) \\ p_{\text{best}} = x \end{cases}$$

where g_{best} is the global best position and p_{best} the personal best solution.
Step 4: If the condition of the previous step is satisfied, g_{best} is set as equal to the best solution otherwise the steps 2-5 are repeated.
Step 5: The values of x and v are updated.
In this study, PSO is utilised to search optimal parameters for the PI controllers of WGS. As mentioned before, the number of PI parameters are 6: (i) 4 parameters for the dq-axis current PI controllers which are K_{pd}, K_{id}, K_{pq} and K_{iq} for the d-axis and q-axis current PI controllers respectively, (ii) 2 parameters for the speed PI controller which are $K_{p\omega}$ and $K_{i\omega}$. The integral parameter K_i of

Table II

COMPARISON BETWEEN PI CONTROLLERS

Parameter	PI tuned by the pole-zero placement method	PI tuned by PSO
K_{pd}	77.410	6.5272
K_{id}	0.4335	0.0141
K_{pq}	77.410	65.100
K_{iq}	0.4335	0.0141
$K_{p\omega}$	0.7035	3.2180
$K_{i\omega}$	0.0542	0.1363

all the controllers (K_{id}, K_{iq}, and $K_{i\omega}$) are calculated as below:

$$k_{pd}s + k_{id} = 0 \bigwedge R_s + L_d s = 0 \Leftrightarrow \frac{R_s}{L_d} = \frac{k_{id}}{k_{pd}}. \quad (20)$$

Therefore, the number of parameters to be optimised is actually 3. In addition, the searching space of each particle is specified in the initialisation step. In the evaluation step, the fitness value of the initial particle set is calculated as below:

$$F = |e_\omega| + OS\% + |e_{id}| + |e_{iq}| \quad (21)$$

where F is the fitness value, e_ω the speed error, e_{id} the d-axis current error, e_{iq} the q-axis current error and $OS\%$ the percentage overshoot of the speed signal which is given as:

$$OS\% = max(\omega_{\max} - \omega_{ss}) \quad (22)$$

where $\omega_{\max}$ is the maximum speed and ω_{ss} the steady-state speed. The optimisation objective is to minimise F in order to make the WGS more stable under rapid wind speed variations. A comparison between the original and optimised PI parameters is listed in Table II.

4. Analysis of Simulation Results

In this research, no-load and load tests have been undertaken in order to calculate the physical parameters of the PMSG (type GL-PMG500A). The following assumptions have been made in experimental tests: the magnetic circuit is assumed linear, (i.e. magnetic saturation is neglected) and the mathematical model is assumed to be without core losses. The parameters of a VAWT and a PMSG used in this simulation are given in Table III. The implemented simulink model of the proposed WGS is shown in Fig. 4. The total-harmonic distortion (THD) for the three-phase line current (Fig. 5) is calculated at low, 7 m/s, rated, 11 m/s, and high, 15 m/s wind speeds which are listed in Table IV. It illustrates that the values of THD for both the HBCC and IPICC techniques are less than 8% that is within the limit of the IEEE 519 standard recommendations on harmonics levels. In addition, it shows that the THD decreases at rated and high wind speeds.

Figure 6 shows the wind turbine performances using the three MPPT control strategies at rated wind speeds. It can be observed in Fig. 7 that the simulated rotational speed tracks the calculated reference speed which ensures

Table III

ACTUAL PARAMETERS OF THE WGS

Parameter	Value
VAWT	
Type	Savonius VAWT
Rated Power	165 (W)
Rated Wind Speed	11 (m/s)
Optimal TSR	0.82
Maximum Power Coefficient	0.22
PMSG	
Type	GL-PMG500A
Rated Power	500 (W)
Stator Winding Resistance	0.35 (Ω)
Moment of Inertia	0.066 (kg.m^2)

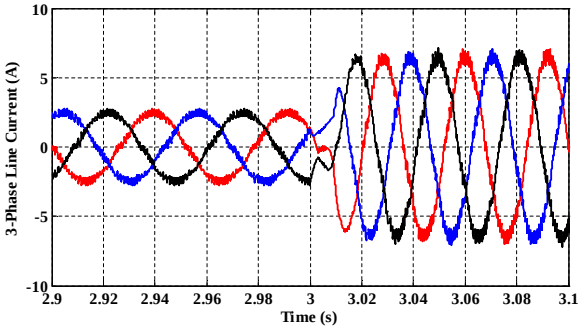

Fig. 5. Three-phase line current responses under wind speed variations from low to rated using the IPICC technique

Table IV

FOURIER ANALYSIS OF THE THREE-PHASE LINE CURRENT OF THE THREE CONTROL TECHNIQUES

Wind Speed	THD (%)		
	HBCC	PICC	IPICC
Low	7.4	7.4	8.8
Rated	5.3	8.3	5.9
High	4.2	18.8	4.1

Table V

DYNAMIC PERFORMANCES OF THE THREE CONTROL TECHNIQUES

Wind Speed	HBCC		PICC		IPICC	
	$OS\%$	t_s (s)	$OS\%$	t_s (s)	$OS\%$	t_s (s)
Low	13.13	0.65	21.3	1.96	13.33	0.74
Rated	11.95	0.65	35.91	3.03	12.46	0.79
High	12.48	0.78	46.84	10.0	13.01	0.80

the optimal TSR, 0.82, and then the maximum power coefficient, 0.221. Table V summarises the dynamic performances which are OS, and t_s of the three MPPT techniques. It is important to note that WGS output power is increased as much as 197% of the the one without using the MPPT controllers. It shows in Fig. 7 that the TSR and the power coefficient are close to their optimal values under wind speed variations which are close to their optimal values.

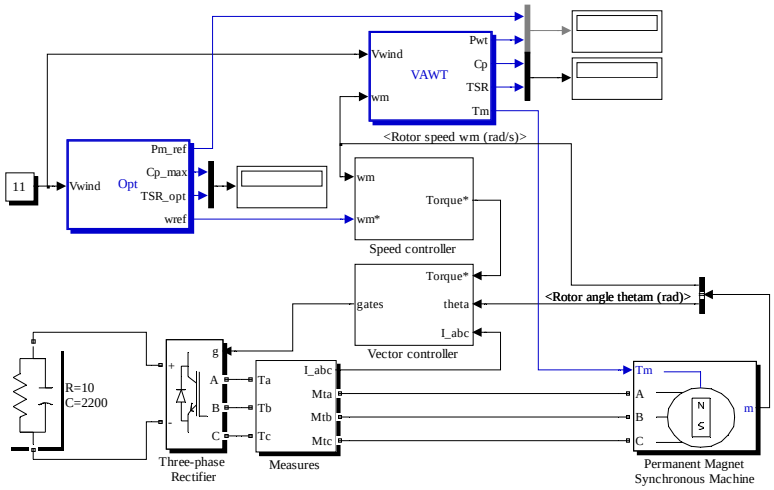

Fig. 4. The implemented simulink model of WGS

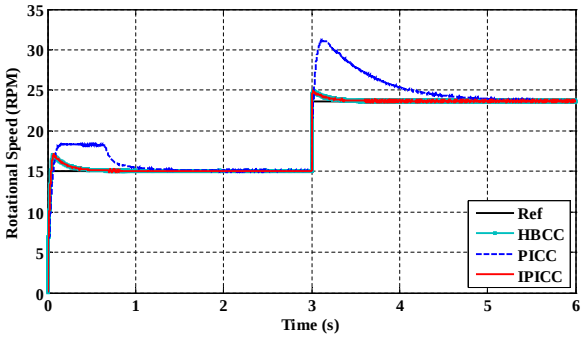

Fig. 6. Rotational speed responses under wind speed variations from low to rated with the proposed techniques

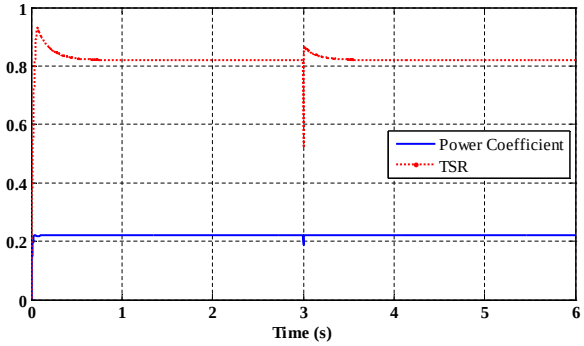

Fig. 7. TSR and power coefficient responses under wind speed variations from low to rated using the IPICC technique

5. Conclusion

In this paper, a small-scale WGS using VAWT and PMSG with a controlled PWM rectifier has been configured a simulation. A comparison among the three current control methods (HBCC, PICC, and IPICC) using the vector control strategy has been undertaken. The results show that the dynamic response performance of the HBCC method is better than the PICC method. It is shown in simulations that the IPICC method has low steady state errors and overshoots compared with the PICC method. It can be concluded that the implementation of PSO for optimising the parameters of the PI controllers is a practical solution compared with conventional PI tuning methods.

References

[1] A. Jamal, D. Venkata, M. Andrew. A review of power converter topologies for wind generators, *Industry Applications Conference*, November 2007, pp. 2369-2385.

[2] R. Datta, and V. T. Ranganathan. A method of tracking the peak power points for a variable speed wind energy conversion system, *IEEE Trans on. Energy Conversion*, vol. 18, no. 1, March. 2003, pp.163-168,

[3] J. Tsai and K. Tan. H APF harmonic mitigation technique for PMSG wind energy conversion system, *IEEE Trans on. Power Engineering*, AUPEC 2007, pp. 1-6.

[4] T. Ackermann. Wind Power in Power System. John Wiley and Sons, 2005.

[5] S. Heir, Grid Integration of Wind Energy Conversion Systems, John Wiley & Sons Ltd, 2nd edition 2006, ISBN 978-0-470-86899-7.

[6] M. Fatu, C. Lascu, G. D. Andreescu, R. Teodorescu, F. Blaabjerg. Voltage Sags Ride-Through of Motion Sensorless Controlled PMSG for Wind Turbines, *IEEE Trans on. Industry Applications*, Sept. 2007, pp. 171-178.

[7] F. Eugene. Electric machinery. McGraw Hill, 2003.

[8] T. Senjyu, T. Shimabukuro, and K. Uezato. Vector control of synchronous permanent magnet motors including stator iron loss, *IEEE Trans on. Power Electronics and Drive Systems*, vol. 1, Feb 1995, pp. 309-314 .

[9] A. Zentai and T. Dab. Improving Motor Current Control Using Decoupling Technique, *Serbia and Montenegro*, Nov. 2005, pp.626-630.

[10] M. Lafoz, I. Iglesias, C. Veganzones, M. Visiers A novel double hysteresis-band current control for a three-levelvoltage source inverter, *IEEE Trans on. Power Electronics Specialists*, vol. 1, 2000, pp. 21-26.

[11] F. Wu, X. Zhang, K. Godfrey, P. Ju. Small signal stability analysis and optimal control of a wind turbine with doubly fed induction generator, *IEEE Trans on. Renewable Energy*, Sept. 2007, pp. 751-760.